Journal Pre-proof

Mechanical and Thermal Properties of Carboxymethyl fibers (CMF)/PVA based nanocomposite membranes

Muhammad Bilal Khan Niazi, Zaib Jahan, Arooj Ahmed, Bushra Uzair, Ahmad Mukhtar, Øyvind Weiby Gregersen

Mechanical and Thermal Properties of Carboxymethyl fibers (CMF)/PVA based nanocomposite membranes

Muhammad Bilal Khan Niazi[a,c*], Zaib Jahan[a,c], Arooj Ahmed[a], Bushra Uzair[b], Ahmad Mukhtar[c] , Øyvind Weiby Gregersen[d]

[a]School of Chemical and Materials Engineering, National University of Sciences and Technology, Islamabad, the Pakistan

[b]Department of Biological Sciences, International Islamic University Islamabad, Islamabad, Pakistan

[c]Department of Chemical Engineering, Universiti Teknologi PETRONAS (UTP), Seri Iskandar, Perak, 32610, Malaysia

[d]Department of Chemical Engineering, Norwegian University of Science and Technology, Norway

*Corresponding author to: m.b.k.niazi@scme.nust.edu.pk (Muhammad Bilal Khan Niazi)

Tel.: +92-51-90855103

Postal address: Department of Chemical Engineering, School of Chemical and Materials Engineering, National University of Sciences and Technology, Islamabad, Pakistan

Graphical Abstract

Surface view of CMF in PVA Matrix
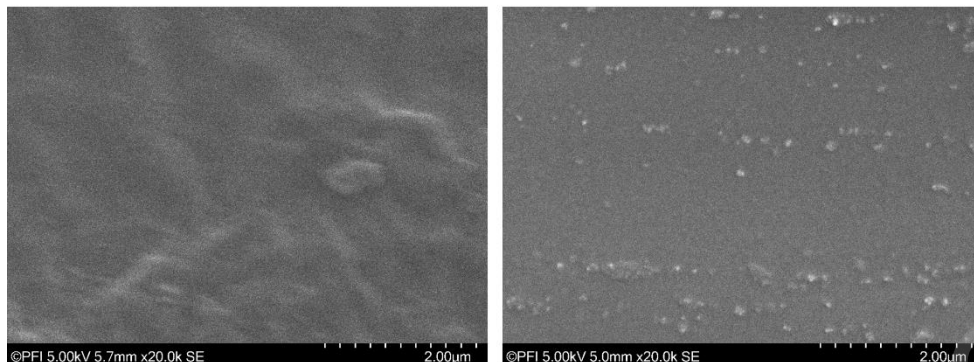
Pure PVA Memebrane   PCMF4(0.08/1.92 g CMF/PVA)

Highlights

- Addition of CMF to swollen PVA at 93%RH increased E-modulus 7 fold.

- The maximum swelling is achieved at low CMF content in PVA matrix.

- Highlight 1 and 2 make PVA-CMF membranes promising for CO2 separation.

- The XRD and FTIR results revealed the good compatibility among PVA and CMF.

- Addition of CMF has no effect of thermal properties of PVA/CMF membranes.

Abstract

Carboxymethyl fibers (CMF) of cellulose are renewable biopolymer and have shown strong reinforcing properties when added to a compatible polymer matrix. The objective of this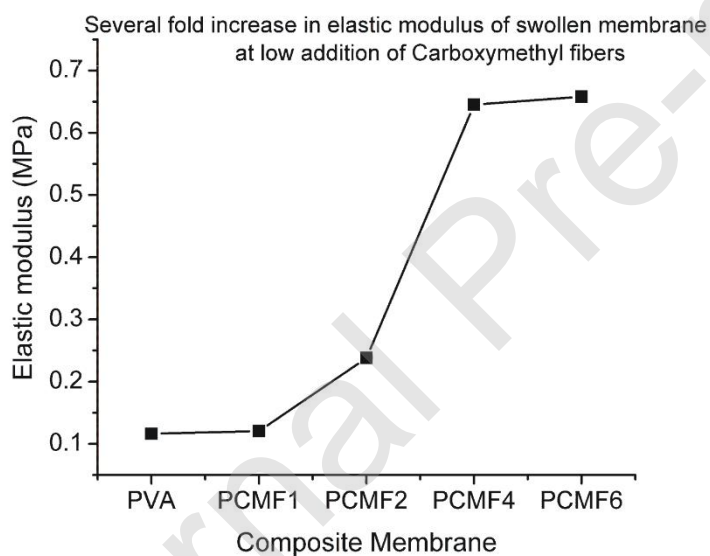 study was to investigate the effect of CMF on the mechanical, thermal and swelling properties of polyvinyl alcohol (PVA) membranes. The PVA/CMF composite membranes with different proportions of CMF ranging from 1 wt. % to 6 wt. % were prepared by solution casting method. The membranes were characterized by SEM, TGA, XRD, FTIR and mechanical testing. The results revealed that at low CMF concentration composite membranes showed homogenous dispersion of CMF in PVA matrix. The incorporation of CMF enhanced the crystallinity of composite membranes with increase in relative humidity (RH). Furthermore, the mechanical strength and moisture uptake of PVA/CMF nanocomposite membranes were enhanced after inclusion of CMF. TGA and DSC results revealed that the addition of CMF has no significant impact on the thermal properties. PVA/CMF nanocomposite membranes showed good potential to be applied for gas separation application particularly for CO_2 capture.

Keywords: Poly(vinyl alcohol); carboxymethyl fibers; Mechanical strength; Dynamic Mechanical properties; Thermogravimetric analysis.

1. Introduction:

Strict environmental regulations have made green processes a huge domain of interest for scientists and engineers. In order to enhance the mechanical properties of the polymeric membranes, number of fillers have been added to polymer matrix. However, to address the global environmental issue in parallel, the use of natural fibers in the composite membranes as reinforcing agent has gained central attention [1-4]. In the past few years, health and environmental controversies have spawned the use of biopolymers [5] and environmentally benign fillers.

Biocompatible, biodegradability, non-toxicity and easy of availability of biopolymers [6, 7] has made them the ideal candidates for substituting petroleum based products [3]. Among the biopolymers, polysaccharides and proteins are most commonly exploited [8]. Polysaccharides like starch [9], chitosan [10], glycogen [11] and cellulose [12] are given special consideration due to their poly-functionality and surface group modification. Moreover, these polymers can easily be fabricated into membranes with dense and porous structure. However, low mechanical strength is an inherent problem with natural polymers that restrict their applications [2]. To overcome this issue and meet the particular process requirements, the addition of nano-fillers into polymeric matrix has shown a great potential [13].

Cellulose is one of the most abundantly availably natural polymers. It has been extensively used in diverse applications such as gas permeations, packaging, water treatment and medical applications (drug release and dialysis). Cellulose is composed of repetitive units of β $(1\rightarrow 4)$ linked D-Glucose. The nano size fibrils of cellulose can be classified as crystalline part and an amorphous part [14, 15]. These crystalline and amorphous regions can be easily extracted by using different techniques [16]. It is biocompatible, biodegradable and low density material with

large number of functional groups present on its surface [17]. It dissolves in various solvents including water, cadmiumethlyenediamine (Cadoxen), cupriethylenediame (CED), N methylmorpholine N oxide and lithium chloride/N,Ndimethylacetamide. One of the very important ionic ether derivatives of cellulose; carboxymethyl fibers (CMF) is a biocompatible and non-toxic material [18]. Owing to its hygroscopic nature, it readily dissolves in hot or cold water and results in a viscous solution [19]. It has ability to interact with other polysaccharides due to carboxylate and hydroxyl functional groups. Hence, it can be used as filler to reinforce the properties of composites. CMF has been verbosely used in textile printing, drug delivery, food, drilling of oil wells, detergents and many others [16, 20]. In addition to hydrophilic hydroxyl and carboxyl groups, it has a hydrophobic backbone making it amphiphilic in nature [21]. However, this research has been conducted to study the improvement in thermal and mechanical properties of Poly(vinyl alcohol) (PVA) membranes incorporated with CMF to be used for gas permeation.

PVA is a biopolymer having good chemical stability and moderate mechanical properties [22]. PVA is hydrophilic polymer containing many hydroxyl groups on its surface that makes it water soluble [23]. Due to its excellent film forming properties and environmental friendly nature, it has been utilized in various applications like membrane technology [24], biotechnology, pharmaceutical applications [4], surgical sutures, packaging [25] and drug delivery [26, 27]. PVA matrix has shown compatibility with various other polymers and fillers and form composites membranes. Thus, it has been widely investigated by the researchers for gas permeation particularly for CO_2 capture [27, 28].

To reinforce the mechanical and thermal properties of PVA, the incorporation of gold [29], silver [30], nano-silica [31], carbon nanotubes [32, 33], clay [1, 34] and hydroxyapatite [35] as fillers

has been reported in literature. All these studies focus on improving the barrier and mechanical properties of PVA employing fillers. However, the mechanical properties should be improved in such a way that its valuable properties are not damaged. Cellulose fibers have been found as potential candidates for this purpose and many studies have shown the improvement in the properties after the addition of cellulose fibers [36-38]. CMF has been used as a filler with different polymers to improve the overall properties of the composite such as pectin [39], starch [40], polycaprolactone [41], polyvinyl alcohol [14], polylactic acid [42]etc.

Keeping this background, the current study was designed to focus on the improvement of mechanical and thermal properties of the PVA membranes by incorporating CMF. The effect of filler concentration on membrane morphology, mechanical and thermal properties has been investigated in detail by using SEM, Universal tensile tester, DSC and TGA, respectively. The crystallinity and molecular interaction were investigated using XRD and FTIR, respectively. The mechanical properties of nanocomposite membranes at high degree of swelling were determined by using tensile testing and DMA. In this perspective, the utilization of such films in the gas separation has been adjudged with respect to their thermal, moisture uptake and mechanical properties.

2. Experiments:

2.1. Materials:

Poly(vinyl alcohol) [MW=89000 Da, 87-89%hydrolyzed] and 2,2,6,6-tetramethyl-piperidin-1-yl) oxyl (TEMPO), sodium hydroxide (NaOH) and Hydrochloric Acid (HCl) was purchased from Sigma Aldrich. Distilled water was used for the experimentation. CMF was prepared in laboratory of Paper and fiber research institute (PFI), NTNU, Trondheim, Norway.

2.2. Preparation of PVA nanocomposite membranes reinforced with CMF:

The Tempo oxidation of pulp method was used without further modifications for the synthesis of CMF as reported in literature by Jonathan Torstensen et. al. [43]. The fresh solution of 1.25% w/w TEMPO pulp and 12.5% w/w NaBr pulp was prepared in deionized water. 220 g of pulp was added to solution and resulting suspension was diluted to 1.33 wt % with slow addition of 1.1 mol NaClO. During oxidation, the pH of suspension was maintained at 10.5. After the completion of oxidation, the suspension was neutralized with 0.5 M HCl followed by the vacuum filtration. At the end, the cellulose and hemicellulose contents were separated by subjecting the suspension to acid hydrolysis. The complete process is available in literature cited above.

To prepare 2 wt% PVA solution, calculated amount of PVA was dissolved in distilled water and mechanically stirred for 3 hours. The mixture was then placed in heating oven at 90 °C for one hour. Afterwards, the solution was kept overnight at mechanical roller to get clear PVA solution. Later, the different proportions of CMF as mentioned in Table 1 were added to PVA solution with subsequent sonication for 24 hours. The resulting homogenous suspensions were then casted into composite membranes by adding equal amounts into petri dishes. The composite membranes were then placed in a closed chamber at atmospheric conditions to ensure constant rate of drying. After drying, the membranes were stored in a desiccator at 0% RH prior further characterization.

Table 1. Material codes and corresponding proportion of PVA/CMF nanocomposite membranes.

Membranes Code	PVA Wt.% solution	CMF (Wt. /Wt.) % of dry PVA
PVA	2 g	0
PCMF1	2 g	1 Wt. %
PCMF2	2 g	2 Wt. %
PCMF4	2 g	4 Wt. %
PCMF6	2 g	6 Wt. %

2.3.   Characterization:

2.3.1. Fourier Transform Infrared spectroscopy (FTIR):

The FTIR analysis was performed to investigate functional groups present in formulated

membranes. Thermo Nicolet Nexus FTIR spectrometer equipped with an attenuated total

reflectance (ATR) device was used for recording the FTIR spectrum of PVA/CMF

nanocomposite membranes. The range of the spectra was recorded in the region of 800-4000 cm^{-1}.

2.3.2. Moisture Uptake:

The moisture uptake of PVA/CMF films under humid conditions at room temperature (23 ^{o} C)

was measure. The 0% RH was attained in a closed chamber. Nanocomposite membranes were

placed in it till they manage equilibrium. Once the equilibrium was established at 0%RH, the

step change in relative humidity (0% RH to 53% RH and 0 % RH to 93% RH) was applied to

nanocomposite membranes. The moisture uptake was recorded periodically for ten days until the

equilibrium was established again with new relative humidity (RH) values, i.e., 53% RH and 93% RH. The gravimetrical analysis of samples was done to calculate the degree of swelling of by using Eq. (1)[44];

$$Moisture\ uptake\ = \frac{Weight_{day,n} - Weight_{day,0}}{Weight_{day,0}}\ x\ 100\% \qquad (1)$$

The subscript 'day, n' represents the weight at the day of measurement, 'day, 0' indicates weight of membrane at equilibrium with 0% RH at 23 ºC.

2.3.3. X-Ray Diffraction (XRD):

XRD pattern was recorded by Bruker D8 Focus X-ray Diffractometer equipped with LynxEye™ super-speed detector and Cu radiations with wavelength of 1.5418 A°. The samples were scanned at rate of 2 s/step and step size 0.02° 2θ. The scan angle was between 10° to 50°.

2.3.4. Scanning Electron Microscopy (SEM):

Hitachi SEM SU 3500 (Japan) was employed to analyze the surface and cross-section morphology of PVA/CMF nanocomposite membranes. Prior to analysis, their surface was sputter coated with gold to avoid the charge accumulation at the surface of the membranes. The acceleration voltage of 5 kV is utilized. The cross sectional analysis was also conducted to investigate the distribution of CMF within PVA matrix. To perform cross sectional analysis, the formulated membranes were soaked in liquid nitrogen to freeze-cracked. The fractured films were sputter-coated with gold layer before analysis [17].

2.3.5. Thermal Analysis:

2.3.5.1. Thermogravimetric Analysis (TGA):

Thermogravimetric analyzer using TGA, Q500 was conducted to investigate the decomposition temperature of formulated nanocomposite membranes. The sample was placed in aluminum pan and heated from 20 °C to 700 °C at a heating rate of 10°C/min. The weight change in relation to temperature was conducted as described in literature [45].

2.3.5.2. Differential Scanning Calorimetry (DSC):

The glass transition temperature (T_g), crystallization temperature (T_c) and melting temperature (T_m) were measured by DSC (TA Q100, Thermal Scientific).The analysis was carried out under N_2 atmosphere from 30 °C to 250 °C at the rate of 10 °C/min. 10 mg of each sample was utilized for DSC analysis. The process consisted of initial heating, then cooling and ultimately second temperature scanning [46].

2.3.6. Mechanical Properties:

2.3.6.1. Mechanical Testing:

The mechanical properties of PVA/CMF nanocomposite membranes were determined by Zwick Roelt Tensile Testing machine. The analysis was carried out according to ASTM D638 standard. Five specimens of each sample were cut into 50 mm in length and 15 mm wide for investigation of tensile strength (TS), % elongation at break (% Eb) and elastic modulus at 25 ºC. The cross head speed was 50 mm/min. Before the analysis, all formulated samples were conditioned for four days at three relative humidities i.e. 0% RH, 53% RH and 93% RH. The experiment was repeated five times.

2.3.6.2. Dynamic Mechanical Analysis (DMA):

The dynamic mechanical analysis was carried out by dynamic Mechanic Analyzer 242 (NETZSCH- Geratebau GmbH) in tensile mode under liquid nitrogen cooling system. The analysis was carried out at a heating rate of 2 C/min and temperature was varied from, -20 °C to 120 °C. The samples dimensions were 5 mm in width and 20 mm length. All formulated samples were conditioned prior to analysis for 4 days at three relative humidities i.e. 0% RH, 53% RH and 93% RH. The thickness of the membranes was also kept constant.

3. Results & Discussion:

3.1.   Fourier Transform Infrared spectroscopy (FTIR):

The FTIR spectra of pure PVA and PVA/CMF nanocomposite membranes are shown in fig 1. In pure PVA, the broad band at 3285.12 cm^{-1} is the stretching vibration of hydroxyl groups in PVA. The stretching vibration of aliphatic CH backbone is shown by peak at 2938.50 cm^{-1}. The band at 1731.81 cm^{-1} corresponds to the stretching vibration of acetate group in PVA. The peak at 1100 cm^{-1} is assigned to CO stretching mode. The bands at 1374.08 cm^{-1} arises due to CH-OH [28]. The peaks related to both PVA and CMF were observed in the formulated nanocomposite membranes. After the incorporation of CMF, the shift in bands of PVA was observed. This shows that the intensity of hydrogen bonding has been increased between PVA and CMF. This evidences the formation of hydrogen bonds between carboxyl and hydroxyl groups present in PVA and CMF [28].The bands appearing at 3283, 3288, 3295, 3297 cm^{-1} in PCMF1, PCMF2, PCMF3 and PCMF4, respectively are due to the OH-stretching vibration in cellulose and PVA. Furthermore, this gives substantial information about the hydrogen bonding [4]. The amorphous nature of cellulose was confirmed by the peaks in the region of 2900 cm^{-1} in PCMF formulations.

No major shift in these peaks was observed that also correspond to the CH stretch. The crystalline band at 1424 cm^{-1} was also present in all formulations with no major shifts with the addition of CMF. The C-O-C linkage of $\beta(1 \rightarrow 4)$ linked D-Glucose appears at 838 cm^{-1}.This band was also present in all the formulations with no major shifts [25].

3.2. Moisture Uptake:

Fig 2 shows the effect of incorporation of CMF to PVA membranes on their moisture uptake ability at different RH; i.e. 53% and 93%. The addition of CMF to PVA membranes showed an increased moisture retention with addition of 1 wt. % of CMF. However, beyond this concentration the moisture retention showed a decreasing trend with increasing amount of CMF. The improvement in swelling behavior of PVA membranes at 1 wt.% of CMF is attributed to the hydrophilic nature of cellulose and its functional group present on the fibril surfaces [46]. However, the decline in degree of swelling beyond 1 wt. % CMF concentration is due to reinforcement effect induced by CMF to PVA matrix. Presence of CMF at higher concentration mechanically restrains the swelling of composite membranes. This can be evident from SEM micrographs shown in section 3.4. At high concentration, PVA/CMF solution has shown reduced stability and CMF form agglomerates. Furthermore, the values of increase in weight percentage of membranes at 93% RH were significantly higher than at 53% RH. Though, the highest and least percentages were attained at the same compositions for both relative humidity values. At 93% RH, the maximum of 37.7 % and lowest 27.2 % was seen in PCMF1 and PCMF6, respectively. However, at 53 % RH the moisture retention values of PCMF1 and PCMF6 are 5.7 % and 3.4 %, respectively. Hence, the membranes swell more at higher relative humidity (93%)

and reinforcement dominates at low values of CMF. Furthermore, it has been observed that the equilibrium was established at the day 5th for all the PVA/CMF membranes on both RH values except the PCMF6 at 53%. PCMF6 at 53% RH showed minimum moisture retention and attained early equilibrium state at the day 4th. The surface activity also enhanced with growing surface area as the proportion of CMF increased in polymer matrix. This can increase the interaction of CMF with available PVA matrix through surface adsorption and hydrogen bonding [47]. Hence, it reduces the moisture uptake and also adversely affects the hydrophilic nature of PVA. Due to this, the percentage weight increased observed for highest addition of CMF (PCMF6) was even lower than the moisture uptake by pure PVA membrane at both RH values [28].

3.3.   X-Ray Diffraction (XRD):

The XRD analysis was carried out to investigate the effect of addition of CMF on the crystallinity of PVA/CMF composite membranes at three different humidities i.e., 0% RH, 53% RH and 93% RH. The diffractogram is shown in Fig 3 (a), (b) and (c), respectively. At 0% RH, the characteristic peak of PVA was observed at 19.5^o that exposed its semi crystalline nature [48, 49]. This peak was still present after the incorporation of CMF. The intensity of this peak was reduced for all the compositions of PVA/CMF membranes. However, a small hump can also been seen for the incorporation of 6 wt. % CMF in addition to PVA peak at all values of RH. At 53 and 93% RH, the same trend was observed; however, the intensity of peak was high as compared to 0% RH.

The CMF is an amorphous polymer with small crystalline regions. The absence of CMF peak at low concentration represents that the CMF structure has large number of amorphous regions

compared to crystalline part [47]. Furthermore, it also shows uniform distribution and stability of

CMF suspensions at low filler concentration. This can also be evident from SEM results in

section 3.4. However, at high CMF concentrations the crystalline region become significantly

high and starts appearing as a shoulder of PVA peak. Furthermore, this decline in peak intensity

can also be attributed to the reduction in inter and intermolecular hydrogen bonding between

PVA and CMF at higher filler concentration [46]. This also shows that as a result of interaction

between hydroxyl groups of cellulose and PVA, the crystallinity of cellulose has destroyed [50].

Moreover, the decreased crystallinity increased the chain flexibility that can be beneficial for

both the gas separation and packaging applications.

3.4.   Scanning Electron Microscopy (SEM):

SEM analysis was carried out to investigate the effect of incorporation of CMF on surface

morphology and thickness of PVA membrane. The surface and cross sectional images were

taken for pure PVA membrane and nanocomposite membranes with different CMF

concentrations. Results are shown in Fig 4. All the casted membranes are found to be dense in

nature. The pure PVA membrane and the membranes with 1 wt. % CMF concentrations showed

smooth and defect free surfaces. That gives visual evidence of uniform distribution of CMF in

PVA matrix. However, with increasing CMF concentration SEM micrographs shows uneven

surfaces with agglomerates present on it. The number and size of these agglomerates enhances

with increased concentration of CMF from 2 wt. % to 6 wt. %. That showed non uniform

distribution of CMF particles in PVA matrix. That refers to non-stability of CMF suspensions in

PVA solution at higher concentration [17]. At low CMF concentrations, there is strong

interaction between the CMF and PVA that caused a uniform dispersion of fibers into the PVA

matrix. However, at higher concentration of CMF the interactions between CMF fibers start

dominating due to the increased number of OH- groups [21]. This reduces the stability of CMF

in polymer matrix. Hence, it appears in form of agglomerates on surface. The uniform dispersion

of fibers in the polymer membrane is crucial in terms of its crystallinity, swelling behavior,

mechanical properties and permeation properties [51].

However, the cross-sectional view of the PVA/CMF membranes shows that the addition of CMF

has the significant effect on the thickness of the nanocomposite membranes. The average

thickness of composite membranes ranges from 94.3 μm to.102 μm.

3.5. Thermal Analysis:

3.5.1. Thermogravimetric Analysis (TGA):

The TGA analysis was performed to investigate the effect of CMF addition on thermal stability

of PVA membranes. The results presented in Fig 5 shows that thermal stability was slightly

improved by addition of CMF. The CMF proportion has direct relation with change in thermal

stability. For cellulosic materials, it is assumed that the thermal behavior is influenced by the

their supramolecular structure [25]. Thermograms showed that the weight of samples decreased

with the increase in temperature. The TGA thermograms show three clear stages of degradation

in PVA and PCMF membranes [52]. The first stage of degradation (up to 110 °C), is associated

with the loss of water and related volatile functional groups [53]. However, it has been observed

that the rate of water loss enhanced with increasing CMF content. The degradation point of PVA

membrane was declined with the addition of CMF. Major weight loss of the PCMF membranes occurred during next two stages of degradation that starts at 230 °C and last until 550 °C till the complete weight lost. More than 50% weight loss of PVA/CMF membranes happened in second stage of degradation. This weight lost is mainly associated with structural degradation of CMF. However, the degradation in last stage is associated with the decomposition of backbone of carbonaceous material [54]. This loss of weight is mainly attributed to the decomposition of polysaccharides present in the nanocomposite membranes [55, 56]. The weight lost here is above 90%. A slight improvement in thermal stability of PVA matrix with the addition of CMF was observed here. The results show that the addition of CMF has no significant contribution in enhancing the thermal properties of PCMF membranes at utilized concentrations.

3.5.2. Differential Scanning Calorimetry (DSC):

The DSC analysis was carried out to investigate the effect of addition of CMF on glass transition temperature (Tg), crystallization temperature (Tc) and melting temperature (Tm) of PVA membrane and results are presented in Fig 6. The DSC analysis clearly shows the three cycles of heating-cooling-heating (H-C-H). The first heating cycle was used to remove thermal history and moisture contents of composite membranes. The small change in Tg was observed with addition of CMF. For semi-crystalline polymers, thermal transition regions could clearly be seen in the thermograms in consistent with literature [46]. It has been observed that the Tg decreased with increased CMF concentration above 1 Wt. %. However, the addition of 1 Wt. % CNC does not show any significant change in Tg of PVA. The Tg of both pure PVA membrane and 1 Wt. % CMF in nanocomposite membranes was observed at 68.9 °C. However, with the gradual increase of CMF up to 2 Wt. % , the Tg decreased to 68.1 °C. The Tg was further decreased with the addition of CMF i.e. with the addition of 4 Wt. % to 6 Wt. % of CMF, the Tg decreased to 65.7

°C and 64.6 °C, respectively. The drop in Tg at the higher content reflects the weak interactions between polymer matrix and filler at higher filler concentrations. The decrease in Tg with addition of higher CMF concentrations is further ascribed to limitation of mobility of PVA chain segments by the adsorptive forces of the CMF. At higher CMF concentrations, filler may offer large surface to form rigid segments at interface [57]. The existence of rigid amorphous factions (RPA) at matrix/fiber interface is often not contributing to Cp change at Tg of the polymer [58]. As a result of these interactions the flexibility and mobility of polymeric chains is reduced, and high temperature would be required to transit from glassy to rubbery state [59]. However, appreciable improvement was detected in crystallization temperature. The crystallization temperature was enhanced with increasing concentration of CMF in PVA nanocomposite membranes. The crystallization temperature for pure PVA membrane was 118.8 °C. However, after the addition of 1 Wt. % CMF, the crystallization temperature increased drastically to 130.7 °C. The maximum crystallization temperature of 157.5 °C was achieved at highest quantity of CMF utilized i.e. 6 Wt. %. The increase in Tc at higher proportions of CMF is due to crystallization as result of heterogeneous phase nucleation. The pure PVA matrix has crystals of uniform shape and size that leads to homogeneous phase nucleation. However, the presence of CMF within PVA matrix reduces the uniformity of crystals and also offer large number of heterogeneous nucleation sites [60]. The characteristic peaks of semi-crystalline polymeric systems in the form of endothermic peaks were clear in all formulation. These peaks are related to the melting of crystalline regions of PVA and CMF as a result of retro degradation[61]. However, the addition of CMF did not affect the melting point of nanocomposite membranes. Slight decrease in the melting point was observed after the addition of 1 Wt. % of CMF in PVA

membranes i.e. 235.1 °C to 234.9 °C. Further addition of CMF in PVA membranes up to 6 Wt. % did not show much change in melting temperature.

3.6. Mechanical Properties:

3.6.1. Tensile Testing:

The tensile properties of PVA and PVA/CMF composite membranes were evaluated at three different humidities i.e. 0% RH, 53% RH and 93% RH. The measured tensile properties were demonstrated in terms of materials tensile strength, elongation at break and tensile modules. The results are presented in fig 7. At 0% RH and 53% RH, the elastic modulus (EM) of PVA membrane show a decline with addition of 1 Wt. % of CMF. However, beyond this concentration EM showed a direct relation with filler concentration at both relative humidities. At 93% RH, the addition of CMF showed increase elastic modulus in all formulated compositions. However, the filler concentration effect on EM is more dominant at high values of relative humidity i.e. 93% RH and 53% RH. Whereas, the value of EM for composite membranes is high at 0% RH as compared to high RH values. This is attributed to high moisture uptake by composite membranes at 53% RH and 93% RH. This can also be ascribed to the interactions between PVA and cellulose due to polysaccharide bonding in cellulose and hydroxyl groups of PVA [61]. Similar results have been reported in literature [62].

Similarly, increasing RH adversely affects the tensile strength (TS). At all three values of RH, no appreciable difference in TS of PVA was observed for addition of CMF up to 2 Wt.%. The addition of 4 Wt. % CMF showed the highest value of the TS, i.e. up to 150 MPa at 0%RH. The high aspect ratio of fillers and high elastic modulus of cellulosic material contributed towards the

increase of tensile strength of composite membranes [63, 64]. The effect is more considerable at high RH when EM of PVA itself decreased due to moisture absorption. CMF is an amorphous material but increase in rigid amorphous fractions (RAF) at PVA matrix /CMF interface at higher CMF concentrations also increases the elastic modulus of composite material. At higher concentrations, large surface area was available for polymer/filler interactions. Fig 7(b) represents the elongation at break (EB) for addition of CMF to PVA matrix. The results showed high values of percentage elongation at higher humidities (53% RH and 93% RH) for all the formulated membranes. The values of percentage EB decreased with increasing concentration of CMF at both 53% RH and 93% RH. However, at 0% RH increasing concentration of CMF does not showed any significant difference in % EB. All the formulated composite membranes showed %EB below 1%. However, at high values of RH all formulated composite membranes showed maximum moisture uptake. It breaks the intermolecular hydrogen bonding and consequence increase in polymer chain flexibility. Hence, by increasing RH the %EB increased and strength of material decreased [57]. The decrease in mechanical properties at higher concentration of CMF (6 Wt. %) is attributed to non-uniform distribution of CMF in PVA matrix. This fact is also in consistent with SEM results.

3.6.2. Dynamic Mechanical Analysis (DMA)

In order to investigate the reinforcing effect induced by addition of CMF in PVA matrix, DMA analysis was conducted at three different RH values. The results are recorded in form of the temperature dependent storage modulus E' and tan δ for all formulated composite membranes as presented in Fig 8. At 0% RH, the E′ of PVA membrane decreases with addition of CMF. However, the highest value was found for addition of 1 Wt. % CMF and addition of 6 Wt.%

CMF showed the lowest value. Furthermore, increase in RH considerably reduces the Tg of all

the formulated membranes. Effect is more dominant at 93% RH where Tg is reduced from 37 $^\circ$C

to -9 $^\circ$C. At 93% RH, the DMA analysis showed scattered results particularly below Tg.

However, an increase in storage modulus was observed with all composite membranes as

compared to pure PVA membrane. The membrane with 4 Wt. % CMF showed the highest value

of elastic modulus at 93 % RH. The value is even higher than pure PVA membrane at 0% RH.

Furthermore, huge drop in storage modulus was observed with respect to increasing temperature.

However, the opposite trend was observed for tan δ. The height of tan δ decreases with addition

of CMF at all values of RH. The additions of cellulose nano fibrils mechanically restrain the

polymeric chain mobility. It reduces the molecular motion of surface adsorbed polymeric chains

and introduces more elastic properties to the material [64, 65]. Whereas, non-uniform

distribution of CMF in PVA matrix and high agglomeration rate at high CMF concentrations

causes a reduction in tan δ. The DMA analysis showed that CMF based composite membranes is

suitable for applications with high moisture contents and high temperature ranges

4. Conclusions:

The study was carried with the aim to investigate the effect of incorporation of nanofiller (CMF)

on mechanical, thermal properties and swelling behavior of PVA/CMF composite membranes. It

has been observed that CMF has reinforcement effect when added to PVA matrix. However, the

proportion of filler and relative humidity play important role in determining the different

properties of composite membranes. The addition of CMF dramatically increased the rate of

moisture uptake of composite membranes. However, increasing CMF concentration reduces the

moisture uptake ability of composite membranes. CMF incorporation has also showed significant

increase in elastic modulus of PVA membranes at high RH. The addition of CMF reduced the

crystallinity of the PVA membranes at 0% RH. However, at high relative humidities i.e. at 53% and 93% RH, crytallinity enhanced with the increase in CMF content. The addition of CMF does not showed any significant improvement in thermal properties of PVA/CMF composite membranes. But, high values of thermal stabilities were found at high relative humidities. The addition of CMF enhanced the mechanical properties of PVA membranes and has potential to be used as reinforcing agent. The SEM images showed uniform distribution of CMF into PVA matrix at low filler concentration. It is concluded that low CMF concentration results in improved mechanical and swelling properties of composite membranes. Hence, addition of 1 wt. % CMF in PVA matrix can be promising solution for membrane application with high RH and high temperatures and pressure conditions. This encourages its usage in applications like gas separations and packaging.

Declarations of interest: none

5. References:

[1] S. Adanur, B. Ascioglu, Journal of industrial textiles, 36 (2007) 311-327.

[2] A. Ahmed, M.B.K. Niazi, Z. Jahan, G. Samin, E. Pervaiz, A. Hussain, M.T. Mehran, Journal of Polymers and the Environment, 28 (2020) 100-115.

[3] S. Esteghlal, M. Niakousari, S.M.H. Hosseini, International journal of biological macromolecules, 114 (2018) 1-9.

[4] M.S. Peresin, Y. Habibi, J.O. Zoppe, J.J. Pawlak, O.J. Rojas, Biomacromolecules, 11 (2010) 674-681.

[5] C. Wang, K. Hu, C. Zhao, Y. Zou, Y. Liu, X. Qu, D. Jiang, Z. Li, M.R. Zhang, Z. Li, Small, 16 (2020) 1904758.

[6] X. Wang, W. Jiang, Q. Zheng, L. Yan, Y. Jin, C. Han, J. Zhuang, H. Liu, Z. Li, small, 11 (2015) 4864-4869.

[7] W. Jiang, H. Li, Z. Liu, Z. Li, J. Tian, B. Shi, Y. Zou, H. Ouyang, C. Zhao, L. Zhao, Advanced Materials, 30 (2018) 1801895.

[8] S. Mohajer, M. Rezaei, S.F. Hosseini, Carbohydrate polymers, 157 (2017) 784-793.

[9] J. Hong, D. An, X.-A. Zeng, Z. Han, X. Zheng, M. Cai, K. Bian, R.M. Aadil, International Journal of Biological Macromolecules, (2020).

[10] N.A. Negm, H.H. Hefni, A.A. Abd-Elaal, E.A. Badr, M.T. Abou Kana, International Journal of Biological Macromolecules, (2020).

[11] T. Guo, Y. Yang, F. Meng, S. Wang, S. Xia, Y. Qian, M. Li, R. Wang, Comparative Biochemistry and Physiology Part C: Toxicology & Pharmacology, (2020) 108709.

[12] A. Khodayari, A.W. Van Vuure, U. Hirn, D. Seveno, Carbohydrate Polymers, 235 (2020) 115946.

[13] G.M. Whitesides, Small, 1 (2005) 172-179.

[14] K. Qiu, A.N. Netravali, Composites Science and Technology, 72 (2012) 1588-1594.

[15] Y.C. Ching, T.S. Ng, BioResources, 9 (2014) 6373-6385.

[16] M. Yadollahi, H. Namazi, Journal of nanoparticle research, 15 (2013) 1563.

[17] Y.C. Ching, A. Rahman, K.Y. Ching, N.L. Sukiman, H.C. Cheng, BioResources, 10 (2015) 3364-3377.

[18] P. Stenius, S.P.-I. Yhdistys, T. Press, F. Oy, Forest products chemistry, Fapet Oy, (2000).

[19] A. Kulikowska, I. Wasiak, T. Ciach, Inżynieria i Aparatura Chemiczna, (2014) 268--269.

[20] M. Yadollahi, H. Namazi, S. Barkhordari, Carbohydrate polymers, 108 (2014) 83-90.

[21] J.-F. Su, Z. Huang, X.-Y. Yuan, X.-Y. Wang, M. Li, Carbohydrate polymers, 79 (2010) 145-153.

[22] D. Huang, B. Mu, A. Wang, Materials Letters, 86 (2012) 69-72.

[23] M.T. Taghizadeh, A. Mehrdad, Ultrasonics sonochemistry, 10 (2003) 309-313.

[24] A. Hussain, M.-B. Hägg, Journal of Membrane Science, 359 (2010) 140-148.

[25] A. Abdulkhani, E.H. Marvast, A. Ashori, Y. Hamzeh, A.N. Karimi, International journal of biological macromolecules, 62 (2013) 379-386.

[26] Y. Tang, Y. Du, Y. Li, X. Wang, X. Hu, Journal of Biomedical Materials Research Part A: An Official Journal of The Society for Biomaterials, The Japanese Society for Biomaterials, and The Australian Society for Biomaterials and the Korean Society for Biomaterials, 91 (2009) 953-963.

[27] K. El- Salmawi, M.A. Zaid, S. Ibraheim, A. El- Naggar, A. Zahran, Journal of applied polymer science, 82 (2001) 136-142.

[28] M.F.A. Taleb, H.A. El-Mohdy, H.A. El-Rehim, Journal of hazardous materials, 168 (2009) 68-75.

[29] J. Bai, Y. Li, S. Yang, J. Du, S. Wang, J. Zheng, Y. Wang, Q. Yang, X. Chen, X. Jing, Solid State Communications, 141 (2007) 292-295.

[30] K.H. Hong, Polymer Engineering & Science, 47 (2007) 43-49.

[31] C. Shao, H.-Y. Kim, J. Gong, B. Ding, D.-R. Lee, S.-J. Park, Materials Letters, 57 (2003) 1579-1584.

[32] J.S. Jeong, J.-S. Moon, S.Y. Jeon, J.H. Park, P.S. Alegaonkar, J.B. Yoo, Thin Solid Films, 515 (2007) 5136-5141.

[33] K.K.H. Wong, M. Zinke-Allmang, J.L. Hutter, S. Hrapovic, J.H. Luong, W. Wan, Carbon, 47 (2009) 2571-2578.

[34] H.M. Ji, H.W. Lee, M.R. Karim, I.W. Cheong, E.A. Bae, T.H. Kim, M.S. Islam, B.C. Ji, J.H. Yeum, Colloid and Polymer Science, 287 (2009) 751-758.

[35] G.-M. Kim, A.S. Asran, G.H. Michler, P. Simon, J.-S. Kim, Bioinspiration & biomimetics, 3 (2008) 046003.

[36] S.S. Laxmeshwar, S. Viveka, D. Madhu Kumar, Dinesha, R. Bhajanthri, G. Nagaraja, Journal of Macromolecular Science, Part A, 49 (2012) 639-647.

[37] A.N. Frone, D.M. Panaitescu, D. Donescu, C. Radovici, M. Ghiurea, M.D. Iorga, Materiale Plastice, 48 (2011) 138-143.

[38] D.M. Panaitescu, D.M. Vuluga, H. Paven, M.D. Iorga, M. Ghiurea, I. Matasaru, P. Nechita, Molecular Crystals and Liquid Crystals, 484 (2008) 86/[452]-498/[464].

[39] G. Agoda-Tandjawa, S. Durand, C. Gaillard, C. Garnier, J.-L. Doublier, Carbohydrate polymers, 87 (2012) 1045-1057.

[40] Y. Wan, H. Luo, F. He, H. Liang, Y. Huang, X. Li, Composites Science and Technology, 69 (2009) 1212-1217.

[41] H. Lönnberg, L. Fogelström, M.A.S.A. Samir, L. Berglund, E. Malmström, A. Hult, European Polymer Journal, 44 (2008) 2991-2997.

[42] L. Suryanegara, A.N. Nakagaito, H. Yano, Composites Science and Technology, 69 (2009) 1187-1192.

[43] J.Ø. Torstensen, M. Liu, S.-A. Jin, L. Deng, A.I. Hawari, K. Syverud, R.J. Spontak, Ø.W. Gregersen, Biomacromolecules, 19 (2018) 1016-1025.

[44] S.D. Zhang, Y.R. Zhang, X.L. Wang, Y.Z. Wang, Starch‑ Stärke, 61 (2009) 646-655.

[45] M.B.K. Niazi, A.A. Broekhuis, European Polymer Journal, 64 (2015) 229-243.

[46] A. Mandal, D. Chakrabarty, Journal of Industrial and Engineering Chemistry, 20 (2014) 462-473.

[47] A. Mandal, D. Chakrabarty, Carbohyd Polym, 134 (2015) 240-250.

[48] A. Joorabloo, M.T. Khorasani, H. Adeli, Z. Mansoori-Moghadam, A. Moghaddam, Journal of Industrial and Engineering Chemistry, 70 (2019) 253-263.

[49] S. Bhowmick, V. Koul, Materials Science and Engineering: C, 59 (2016) 109-119.

[50] X. Zhang, J. Zhu, X. Liu, Macromolecular research, 20 (2012) 703-708.

[51] W. Zhang, X. Yang, C. Li, M. Liang, C. Lu, Y. Deng, Carbohydrate Polymers, 83 (2011) 257-263.

[52] S. Gupta, T.J. Webster, A. Sinha, Journal of Materials Science: Materials in Medicine, 22 (2011) 1763-1772.

[53] M. Galdeano, M. Grossmann, S. Mali, L.A. Bello-Perez, M. Garcia, P. Zamudio-Flores, Materials Science and Engineering: C, 29 (2009) 492-498.

[54] X. Luo, J. Li, X. Lin, Carbohydrate Polymers, 90 (2012) 1595-1600.

[55] A. Nada, M.L. Hassan, Polymer Degradation and Stability, 67 (2000) 111-115.

[56] N. Bhatt, P. Gupta, S. Naithani, Carbohydrate polymers, 86 (2011) 1519-1524.

[57] N. Ninan, M. Muthiah, I.-K. Park, A. Elain, S. Thomas, Y. Grohens, Carbohydrate polymers, 98 (2013) 877-885.

[58] E. Zuza, J.M. Ugartemendia, A. Lopez, E. Meaurio, A. Lejardi, J.-R. Sarasua, Polymer, 49 (2008) 4427-4432.

[59] D. Droste, A. Dibenedetto, Journal of Applied Polymer Science, 13 (1969) 2149-2168.

[60] M.A.S.A. Samir, F. Alloin, J.-Y. Sanchez, A. Dufresne, Polymer, 45 (2004) 4149-4157.

[61] B. Ghanbarzadeh, H. Almasi, A.A. Entezami, Innovative food science & emerging technologies, 11 (2010) 697-702.

[62] X. Ma, P.R. Chang, J. Yu, Carbohydrate Polymers, 72 (2008) 369-375.

[63] M.B.K. Niazi, Z. Jahan, S.S. Berg, Ø.W. Gregersen, Carbohydrate polymers, 177 (2017) 258-268.

[64] H. Dong, Y.R. Sliozberg, J.F. Snyder, J. Steele, T.L. Chantawansri, J.A. Orlicki, S.D. Walck, R.S. Reiner, A.W. Rudie, ACS applied materials & interfaces, 7 (2015) 25464-25472.

[65] O. Chaabouni, S. Boufi, Carbohydrate polymers, 156 (2017) 64-70.

Fig. 1. FTIR Spectra of PVA and PVA/CMF nanocomposite membranes
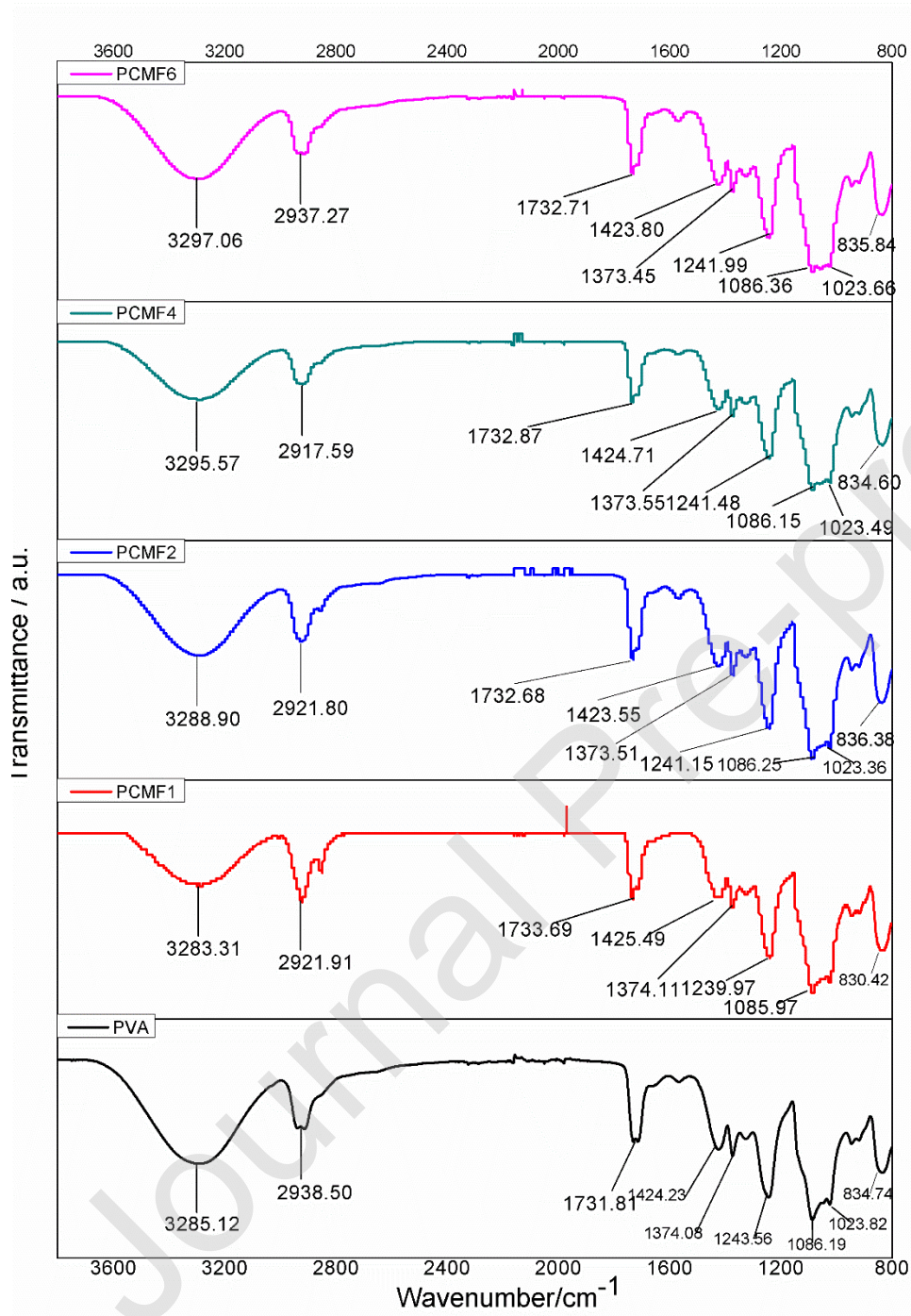
Fig. 2. Moisture Uptake of PVA and PVA/CMF membranes at (a) 53% RH (b) 93% RH
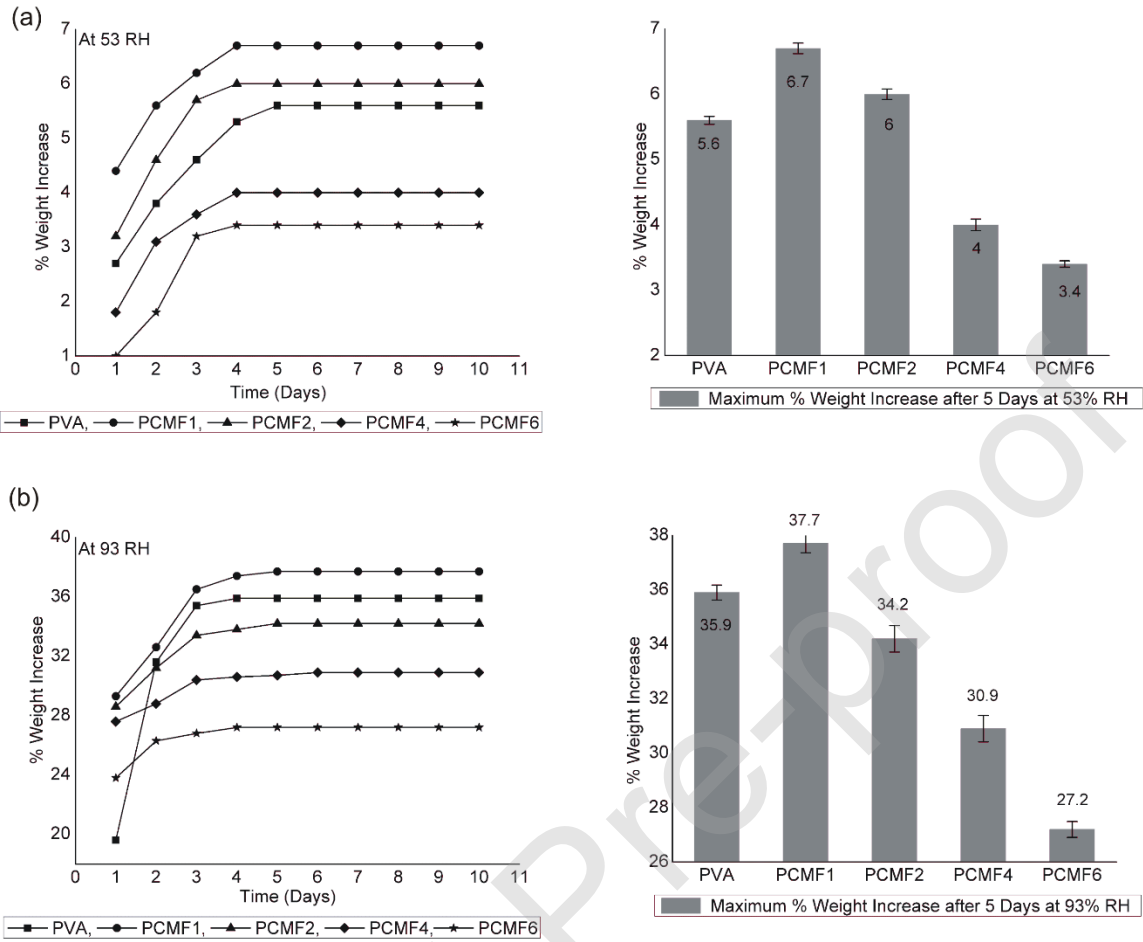
Fig. 3. X-ray diffraction patterns of PVA/CMF membranes at (a) 0% RH (b) 53% RH (c) 93% RH
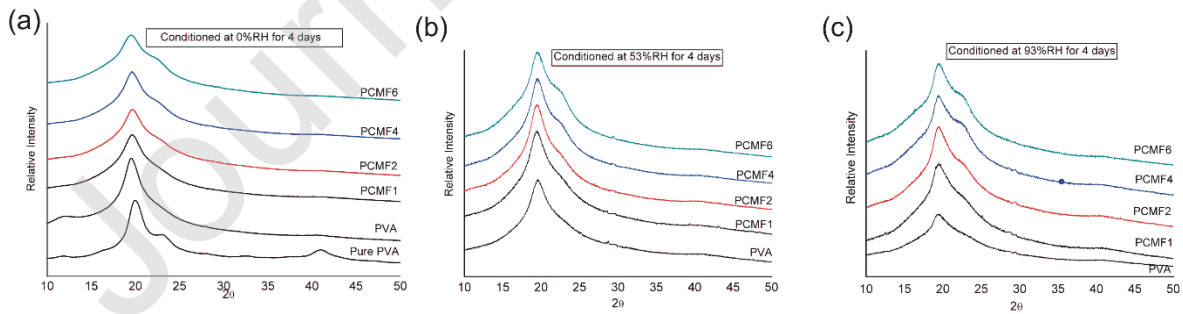
Fig. 4. Scanning Electron Micrographs of PVA/CMF membranes (a) PVA, (b) PCMF1 (c) PCMF4 (d) PCMF6
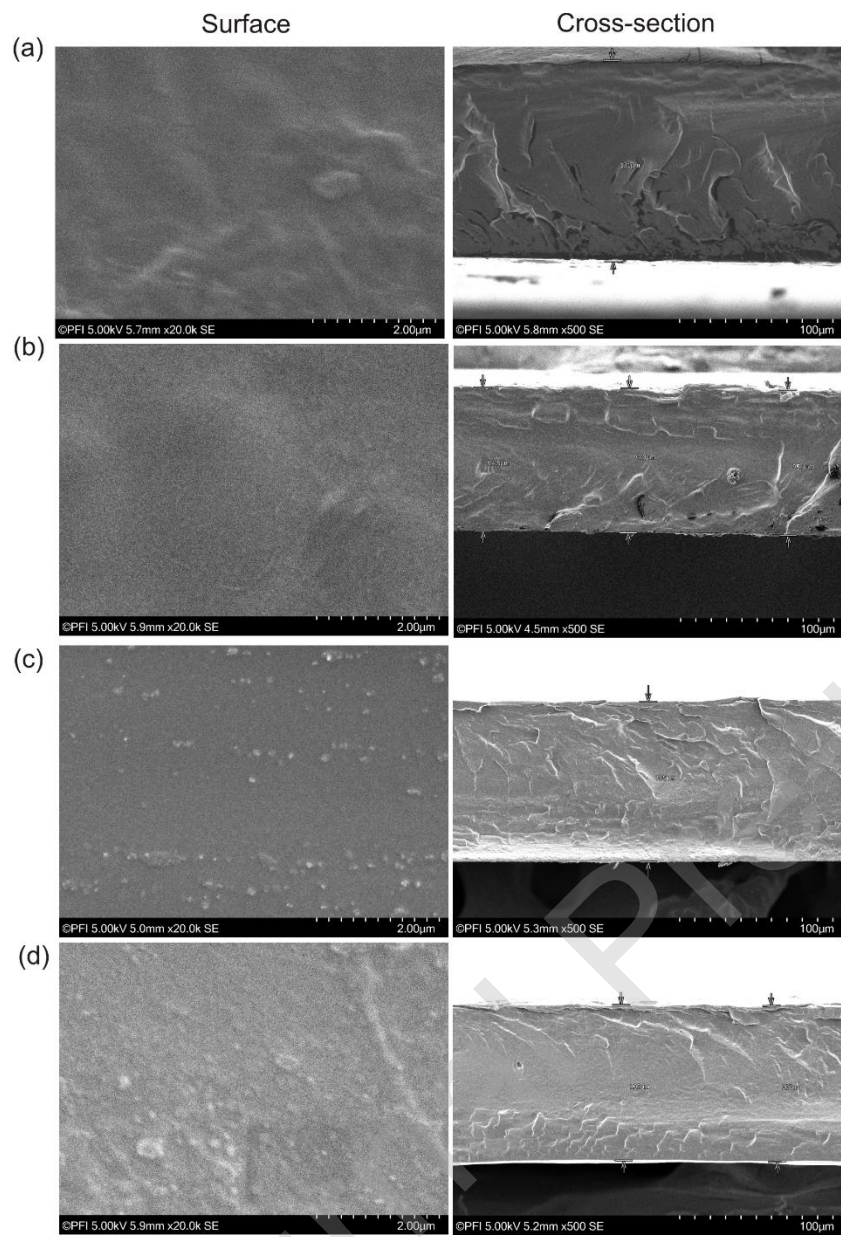
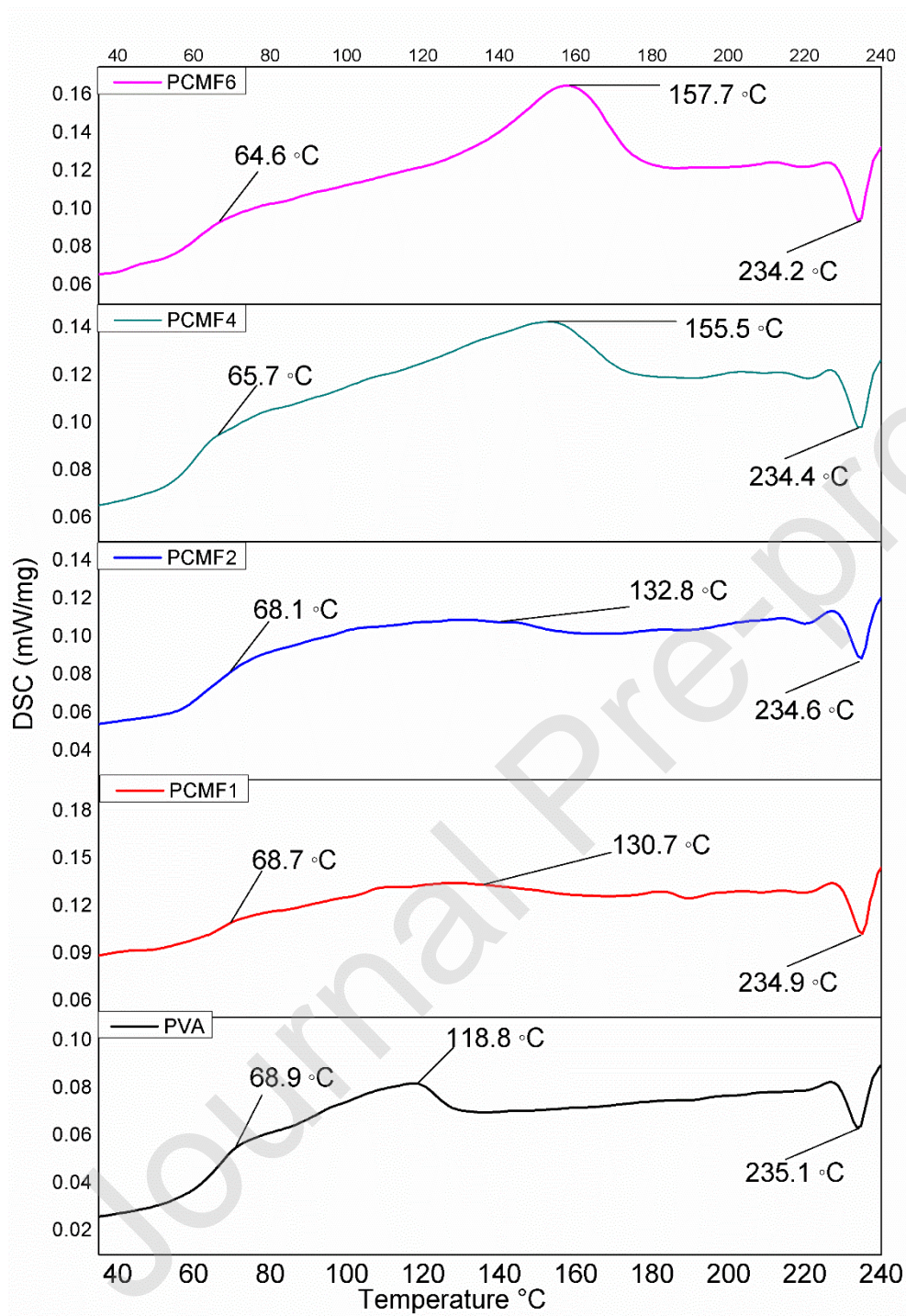Fig. 5. TGA and DTGA curves of PVA/CMF composite membranes.
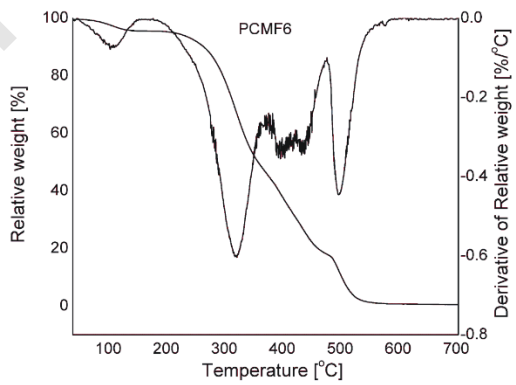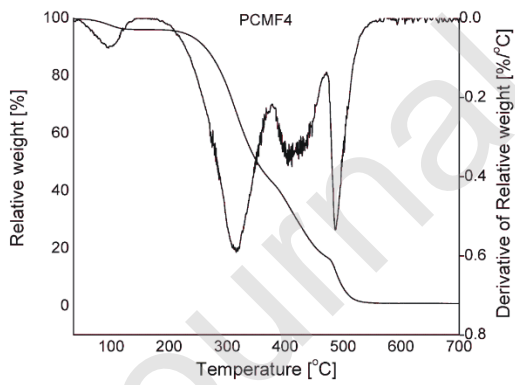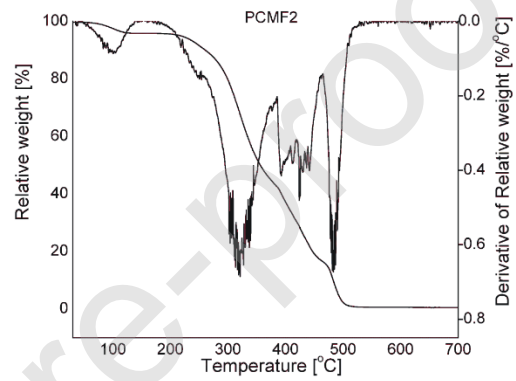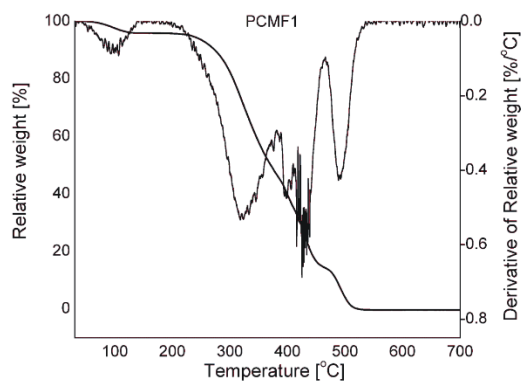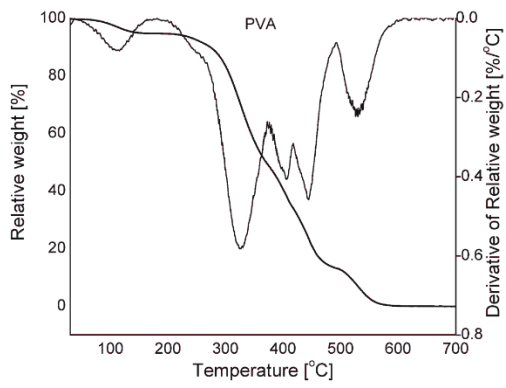
Fig. 6. DSC curves of PVA/CMF composite membranes.

Fig. 7. Mechanical properties of PVA/CMF composite membranes at 0%RH, 53% RH and 93%

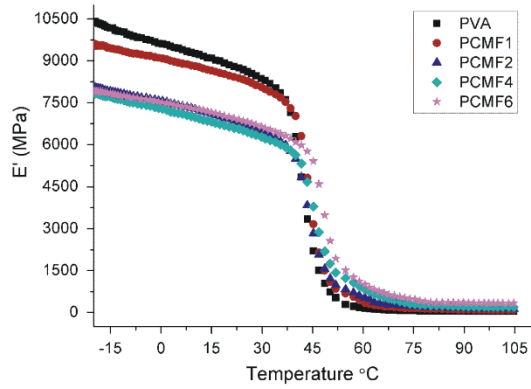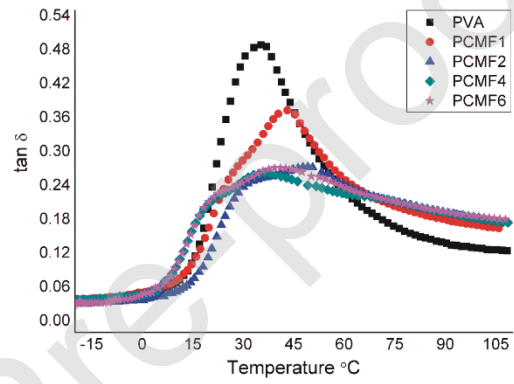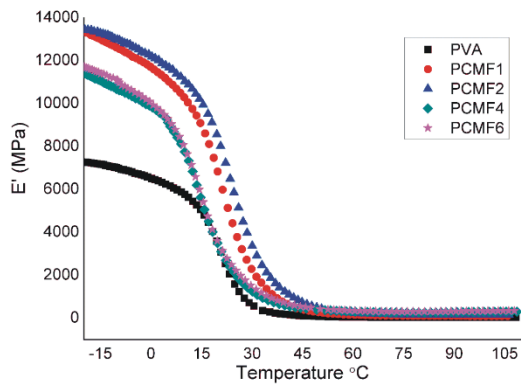RH a) Elastic modulus, b) Tensile strength, c) Elongation at break.
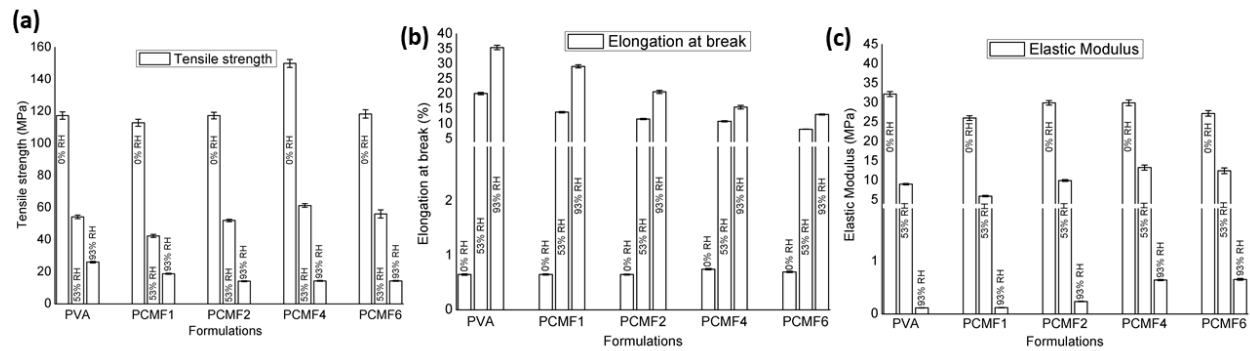
Fig. 8. Dynamic mechanical analysis curves of PVA/CMF composite membranes at a) Storage modulus and tan δ at 0% RH, b) Storage modulus and tan δ at 53% RH and c) Storage modulus and tan δ at 93% RH

(a) 0% RH

(b) 53% RH

(c) 93% RH